

Published in final edited form as:

Inflamm Bowel Dis. 2010 May ; 16(5): 743–752. doi:10.1002/ibd.21148.

A Novel Model of T_H2-polarized Chronic Ileitis: The SAMP1 Mouse

Eoin N. McNamee, PhD^{*}, Joshua D. Wermers, BA^{*}, Joanne C. Masterson, PhD[†], Colm B. Collins, PhD^{*}, Matthew D.P. Lebsack, BSc^{*}, Sophie Fillon, PhD[†], Zachary D. Robinson, MSc[†], Joanna Grenawalt, BSc[†], James J. Lee, PhD[‡], Paul Jedlicka, MD, PhD[§], Glenn T. Furuta, MD[†], and Jesús Rivera-Nieves, MD^{*}

^{*}Mucosal Inflammation Program, Division of Gastroenterology, University of Colorado Health Sciences Center, Denver

[†]Gastrointestinal Eosinophilic Disease Program, Section of Pediatric Gastroenterology, Hepatology and Nutrition, The Children's Hospital, School of Medicine, University of Colorado, Denver

[§]Department of Pathology, University of Colorado, Denver

[‡]Division of Pulmonary Medicine, Department of Biochemistry and Molecular Biology, Mayo Clinic Arizona, Scottsdale, Arizona

Abstract

Background & Aims—SAMP1/Yit mice develop spontaneous, segmental, transmural ileitis recapitulating many features of Crohn's disease (CD). The ileitic phenotype may have arisen during crosses of SAMP1 mice selected for the presence of skin lesions. We hereby describe that the original SAMP1 strain similarly develops ileitis. Our aim was to characterize the histopathological and immunological features of this model and assess its responsiveness to standard IBD therapy.

Methods—The time course of histopathological features of ileitis was assessed. Immune compartments were characterized by flow cytometry. Ileal cytokine profiles and transcription factors were determined by real-time RT-PCR. Finally, response to corticosteroid therapy and its effect on immune compartments and cellularity was evaluated.

Results—Histological features and time course of disease were conserved, compared to those reported in SAMP1/Yit strains, with similar expansion of CD19⁺, CD4⁺ and CD8⁺ effector (CD44^{high}CD62L^{low}), and central memory lymphocytes (CD44^{high}CD62L^{high}). However, different from SAMP1/YitFc mice, analysis of ileal cytokine profiles revealed initial TH1 polarization followed by TH2-polarized profile accompanied by prominent eosinophilia during late disease. Lastly, corticosteroids attenuated ileitis resulting in decreased lymphocyte subsets and cellularity of compartments.

Conclusions—Here we report that the ileitic phenotype of SAMP1-related strains was already present in the original SAMP1 strain. By contrast the cytokine profile within terminal ilea of SAMP1 is distinct from the mixed TH1/TH2 profile of SAMP1/YitFc mice during late disease, as it shows predominant TH2 polarization. Dissemination of these strains may advance our understanding of CD pathogenesis, which in 60% of patients involves the terminal ileum.

Correspondence: Jesús Rivera-Nieves, Mucosal Inflammation Program, University of Colorado Health Sciences Center, East 19th Ave. 12700, MS B-146, RC2 Bldg Rm. 10026, Aurora, CO 80045. Tel: 303-724-7248. Fax: 303-724-7243, jesus.rivera-nieves@ucdenver.edu.

Financial Disclosures: No conflicts of interest exist

Introduction

In 1932 Crohn and colleagues described a chronic disease of young adults involving the terminal ileum (1). Almost 80 years later we still lack an explanation for this particular localization, but it is likely that the relationships between the heavy bacterial load (10^9 CFU) and immune-rich environment of the terminal ileum are key contributors. The inflammatory process described by Crohn was segmental, transmural and accompanied by marked thickening of the muscularis propria. Inflammation within that segment was then attributed to *M. tuberculosis*, yet no infectious etiology could be identified(1).

Since then, many animal models of inflammatory bowel disease (IBD) have been described (2–4). Yet most IBD models affect the large intestine rather than the small bowel, are generated by chemical, immunologic or genetic manipulation and are self-limited in nature. Although these colitic models have greatly expanded our understanding of the pathogenesis of the disease, few really recapitulate the features of the inflammatory process described by Crohn (transmural, segmental chronic inflammation). Furthermore, even fewer exhibit chronic inflammation localized to the terminal ileum, as was present in all original cases described by Crohn(1).

This changed eleven years ago when Matsumoto described a senescence-accelerated mouse (SAM)P1/Yit strain which developed spontaneous ileitis, while losing its accelerated senescence phenotype(5). The SAMP1/Yit strain was generated by crossing SAMP1 mice, selected for the presence of skin lesions. SAMP1 mice were obtained from Dr. Toshi Takeda, who developed the strain from AKR/J mice while studying the genetics of aging(6). Since Matsumoto's original description, it was believed that the ileitic phenotype appeared during these crosses. To ascertain whether this was the case, we obtained the original SAMP1 mice from Dr. Takeda and evaluated their terminal ilea for the presence of ileitis. Unexpectedly, the SAMP1 strain, like its derivative substrains (i.e. SAMP1/Yit, SAMP1/YitFc, SAMP1/YP), also develop terminal ileitis, phenotypically indistinguishable from that of other SAMP1/Yit strains. The selection of mice with skin lesions did not appear to have contributed to the appearance of the ileitic phenotype, as has been previously believed(7).

In the present study, we performed a longitudinal study of the histological and inflammatory characteristics of ileitis in SAMP1 mice. Unexpectedly, different from the mixed T_H1/T_H2 ileal cytokine profile observed during advanced disease in SAMP1/Yit mice, SAMP1 mice exhibited prominent T_H2 polarization after 20-weeks-of-age. Due to the increases in IL-5 and IL-13 transcripts within their chronically inflamed ilea, we assessed for eosinophilic infiltration by immunohistochemistry. Finally, we assessed whether the ileitis of SAMP1 mice responds to corticosteroid therapy.

Materials & Methods

Mice

SAMP1 (SAMP1/SkuSlc) female mice 4- to 20-weeks-of-age were purchased from Japan SLC, Inc. (Hamamatsu, Japan). AKR mice (AKR/J; *a/a Tyr^c/Tyr^c Soat1^{ald}/Soat1^{ald} hid/hid*), from which SAMP strains were derived were purchased from the Jackson Laboratory (Bar Harbor, ME) to serve as controls. All animals were maintained under micro-isolator conditions. Food and water were available *ad libitum*. Fecal samples were negative for *Helicobacter hepaticus* and *bilis* and other murine *Helicobacter* species, and for protozoa and helminths. All animal procedures were approved by the Institutional Committee for Animal Use of the University of Colorado, Denver.

Tissue Collection and histological analyses

The distal ilea (10 cm) were fixed in 10% buffered formalin, paraffin-embedded, cut into 5 μm sections and stained with hematoxylin/eosin. Histological assessment of ileal inflammation was performed using a standardized semi-quantitative scoring system, as described(8). Briefly, scores were given for 3 histologic parameters: (1) active inflammation (granulocyte infiltration); (2) chronic inflammation (lymphocytes, plasma cells, and macrophages in the mucosa and submucosa); and (3) villus distortion (flattening and/or widening of normal villous architecture). Scoring was performed by a pathologist (PJ), blinded to the time point, strain and treatment groups.

Lymphocyte Isolation

Single-cell suspensions were obtained by passing the spleen or MLN through a 100 μm cell-strainer. Red blood cells were lysed by 5 minute incubation in lysing reagent (BD Pharm Lyse, BD Biosciences, San José, CA). The cell suspension was pelleted by centrifugation and re-suspended in complete medium (RPMI 1640 with 10% fetal bovine serum, 2 mmol/L L-glutamine, and 1% penicillin/streptomycin).

Flow Cytometry

Cells from indicated compartments were incubated with fluorescently-labeled antibodies against: mouse CD4 (GK1.5), CD19 (1D3), L-selectin (MEL-14) (BD Biosciences, San José, CA), CD8 (53-6.7), CD8 (Ly-3), CD44 (IM7) (Biolegend, San Diego, CA), TCR (H57-597), (BD Pharmingen) or corresponding isotype controls. Cells were fixed with 2% paraformaldehyde and 7-color analyses were performed using the BD FACSCanto™ II (BD Biosciences, San Jose, CA). Further analyses were performed using FLOWJo software (Tree Star Inc, Ashland, OR).

Real-Time RT-PCR

Total RNA was isolated from homogenized ilea using the RNeasy Mini Kit (QIAGEN, Valencia, CA). RNA samples (1 μg) were reverse transcribed into cDNA with a high capacity cDNA archive kit (Applied Biosystems, Foster City, CA) and Real-time PCR performed using an ABI Prism 7300 instrument. Taqman Gene Expression Assays (Applied Biosystems, Foster City, CA) containing primers and a FAM™ dye-labeled TaqMan® MGB probes were used to quantify genes of interest. Assay designations were as follows: IL-5 (Mm99999063_m1), IL-13 (Mm00434206_g1), TNF (Mm00443258_m1), IFN- (Mm00801778_m1), GATA3 (Mm01337569_m1) and T-bet (Mm00450960_m1). PCR was performed in a 20 μl reaction volume (9 μl of diluted cDNA, 1 μl of Taqman gene expression assay and 10 μl of Taqman® Universal PCR Master Mix). PCR was performed in duplicate, using universal cycling conditions per manufacturer's instructions (Applied Biosystems, Foster City, CA). Thermocycling conditions were: 95°C for 10 minutes, 40 cycles of 95°C for 15 seconds, and 60°C for 1 minute. 18S was used as endogenous control to normalize gene expression data, and an RQ value ($2^{-\text{DDCt}}$, where Ct is the threshold cycle) was calculated for each sample using ABI RQ software (Applied Biosystems, Foster City, CA). RQ values are presented as fold change in gene expression relative to the control group.

Major basic protein (MBP) immunostaining

MBP immunostaining was performed as previously described(9). Briefly, 5- μm sections were quenched with H₂O₂, blocked with normal goat serum, and stained with rabbit anti-murine eosinophil MBP antisera. Slides were washed and incubated with biotinylated goat anti-rabbit antibody and avidin-peroxidase complex (Vectastain ABC Peroxidase Elite kit; Vector Laboratories, Burlingame, CA), developed by nickel diaminobenzidine, enhanced with cobalt chloride and counterstained with methyl green. Quantification of

immunoreactive cells was performed using NIS-Elements Imaging Software (Nikon Microscopes, Melville, NY). Seven images were acquired and assessed from randomly selected locations of each ileal section (n=5/strain and age/group). Eosinophils were quantified using the standard area measurement (S.A.M.) technique. Briefly, the area occupied by an eosinophil was assessed and the S.A.M determined for a single eosinophil. The total MBP-positive area was determined for each field and divided by the S.A.M. to obtain the number of eosinophils per high power field.

Corticosteroid treatment

11-week-old SAMP1 mice received 4 intraperitoneal (I.P.) injections of 100µg dexamethasone (VEDCO, St. Joseph, MO) or saline vehicle every other day for 8 days. Tissue was harvested 24 hours after the last injection.

Statistical Analysis

Statistical analyses were performed using the two-tailed Student's *t*-test. Data were expressed as mean ± standard error of the mean (SEM). Statistical significance was set at *P* < 0.05.

Results

Histological progression of SAMP1 ileitis

Ileal inflammation was not observed in SAMP1 or AKR mice at 5-weeks-of-age. Histologic examination of the esophagus, stomach, duodenum, jejunum, cecum and colon revealed no inflammation (not shown). However, by 10-weeks-of-age, SAMP1 mice displayed significant ileitis (Figure 1A, B). All indices increased (villus distortion, active, chronic, total) compared to AKR (mean ± S.E.M. from 5-to 50-weeks-of-age) and 5-week-old SAMP1 (villus distortion: 3.2 ± 0.6 , *P* < .001; active: 2.5 ± 0.5 , *P* = .002; chronic: 3.6 ± 0.9 , *P* = .006; total: 9.6 ± 2 , *P* < .002) (Figure 1A). Between 10- and 50-weeks-of-age there was progression of the severity of villus distortion and active inflammation reaching a maximum of 6.2 ± 0.8 and 6.3 ± 0.7 respectively. Histological hallmarks of disease included transmural, mixed inflammatory infiltrates from the mucosa to the serosa. Chronically-inflamed 20-week-old and older mice additionally exhibited crypt elongation, lymphoid aggregates, rare giant cells and further progression of transmural infiltrates, accompanied by blunting of the villi, crypt and goblet cell hyperplasia (Figure 1B)

Expanded lymphoid compartments in SAMP1 mice

At 5-weeks-of-age, while no histological evidence of ileitis was identified, significant expansion of splenic cellularity was observed (Figure 2A & B). By 20-weeks-of-age, there was further expansion in the cellularity of the MLN and spleen (Figure 2A). Further compartment flow cytometric analysis revealed increased absolute numbers of CD4⁺, CD8⁺ and CD19⁺ lymphocytes compared to AKR controls at 20-weeks-of-age in both MLN and spleen (Figure 2C & D). As observed in the SAMP1/Yit mice, a large increase in the numbers CD4⁺ and CD8⁺ lymphocyte subpopulations was observed, compared to AKR controls (10) (Table 1).

Increased effector and central memory T lymphocytes correspond with severity of SAMP1 ileitis

Further characterization of 5-week-old AKR and SAMP1 splenocytes revealed significant differences in both T_{EM} and T_{CM} within the CD8⁺ subset (*P* = .02, *P* = .03 respectively) and for T_{EM} within the CD4⁺ population (CD4⁺ *P* < .0001). Analysis of the SAMP1 MLN at 5-weeks-of-age displayed significant expansion of T_{CM} compared to AKR mice (*P* < .0001).

While there was no significant increase in SAMP1 CD4⁺ T_{EM} within the MLN by 20-weeks-of-age (Figure 3, upper panel), all other populations in MLN and spleen were markedly increased, corresponding with worsening disease (AKR vs. SAMP1; P<.05; Figure 3, lower panels).

Early and late disease are characterized by distinct T_H1 and T_H2 cytokines profiles in the SAMP1 ileum

Cytokine profiles of the SAMP1 ileum revealed T_H1 polarization with significant fold increases in the expression of IFN- and TNF mRNA at 5 and 10 weeks. Conversely, a distinct T_H2 expression profile characterized late disease (>20-weeks-of-age) as both TNF and IFN- decreased to basal levels, while the levels of IL-5, IL-13 and IL-10 were significantly up-regulated (Figure 4).

Expression of transcription factors Tbet and GATA3 correspond to cytokine profiles in early and late ileitis

The expression of transcription factors which orchestrate T_H1 and T_H2 cell polarization, Tbet and GATA3, were assessed in ilea. Greater expression of Tbet predominated during early disease in SAMP1 mice (5 weeks; Tbet 0.75 ± 0.2 vs. 2.5 ± 0.5, P<.005; GATA3, 0.6 ± 0.1 vs. 1.62 ± 0.2, P=.002). Consistent with the pronounced expression of IL-5, IL-13 and IL-10 during chronic disease, the ratio of GATA3 expression was significantly elevated compared to Tbet in SAMP1 ileum by 50-weeks-of-age (GATA3/Tbet ratio: 50 weeks 1.34 ± 0.21 vs. 5.9 ± 1.1, P<.007) (Figure 5).

Increased eosinophilic infiltrates distinguish late ileitis in SAMP1 mice

To further define the T_H2 inflammatory milieu, we performed additional cellular characterization of ilea of AKR and SAMP1 mice. As eosinophilic infiltration is difficult to assess with traditional staining methods, we utilized immunohistochemical staining with anti-major basic protein (MBP) antibody. Quantification of eosinophils of SAMP1 ileal tissue revealed a marked increase in eosinophil numbers by 20-weeks-of-age, compared to AKR mice (5 week SAMP1 vs. 20 week SAMP1: 2.6 ± 0.4 vs. 51 ± 10, P=.004) (Figure 6A) coinciding with increased IL-5 and IL-13 expression (Figure 4). Representative MBP-stained tissue sections from 20-week-old SAMP1 displayed prominent ileal eosinophilic infiltrates from the muscularis to the villus tips (Figure 6B).

Therapeutic treatment with corticosteroids

As corticosteroids are clinically proven to treat flares of CD, we assessed the effects of dexamethasone (Dex) on the severity of SAMP1 ileitis. Treatment of 11-week-old SAMP1 mice led to marked attenuation of ileitis, as evidenced by significant reduction in MLN and spleen cellularity and inflammatory indices (Vehicle vs. Dex: Active: 1.2 ± 0.2 vs. 0.14 ± 0.1, P=0.003, chronic: 1.4 ± 0.2 vs. 0.05 ± 0.03, P=.002, total: 4.8 ± 0.5 vs. 0.5 ± 0.3, P=.002). Dexamethasone treatment also significantly restored villus architecture (vehicle vs. Dex: 1.6 ± 0.4 vs. 0.1 ± 0.1, P=.004) (Figure 7A). In addition, other histological hallmarks of disease: muscularis propria, goblet and paneth cell hyperplasia, were diminished (Figure 7B). Marked reduction in lymphocyte counts in MLN (vehicle vs. Dex: 90.7 ± 6.8 vs. 30 ± 0.4, P=.004) and spleen (161.7 ± 4.2 vs. 53.2 ± 5.4, P<.0001) were observed. Dexamethasone treatment decreased IFN- (vehicle vs. Dex: x 4.9 ± 1.4 vs. x 0.8 ± 0.2, P=.002) and TNF (vehicle vs. Dex: x 2.9 ± 0.9 vs. x 0.8 ± 0.1, P<.002) mRNA levels in SAMP1 ilea, which were comparable to that of uninfamed AKR controls. Taken together these results demonstrate that SAMP1 ileitis responds to standard therapy used in CD.

Discussion

Eleven years after the description of the first mouse model of spontaneous, segmental, transmural Crohn's-like ileitis (i.e. SAMP1/Yit)(5), access to this unique resource has been limited. In the present report we characterize a novel commercially available SAMP strain (SAMP1) that, like its related strains, (i.e. SAMP1/Yit(5), SAMP1/YitFc(10), and SAMP1/YP(11)) develops spontaneous segmental, transmural ileitis with 100% penetrance. Similar to the SAMP1/YitFc strain, mice develop near maximal disease by 10-weeks-of-age with increased size and cellularity of lymphoid compartments and expansion of effector and central memory T cell subsets. By contrast the cytokine profile within the inflamed terminal ilea of SAMP1 is distinct from the mixed T_H1/T_H2 profile of SAMP1/YitFc mice during late disease, as it shows a predominant T_H2 polarization(12). Furthermore, SAMP1 ileitis responds dramatically to corticosteroids, with near resolution of ileitis and marked reduction of the cellularity of lymphoid compartments.

Few animal models develop spontaneous IBD (e.g. Cotton Top Tamarins(13), C3H/HejBir(14) and SAMP1 strains(5)). The original SAMP strains were developed by Dr. Toshio Takeda after over 24 brother-sister matings of AKR mice obtained from The Jackson Laboratory (Bar Harbor, Maine, USA)(6). The authors reported alopecia, loss of activity and shortened life span, among other phenotypic features(5). Sub-strains of these mice were termed "senescence accelerated mouse", and later, (SAM)P to denote "senescence-prone" variants. Five separate series of the strain were further divided into SAMP-1, -2, -3, -4 and -5(6). The SAMP1/Yit model of ileitis, described by Matsumoto and colleagues, was developed by continuous brother-sister mating of SAMP1 mice displaying skin lesions, which correlated with the presence of intestinal inflammation(5). Although the precise cause of ileitis in these mice is still unknown, it is likely that as in CD, genetic and environmental factors (such as the bacterial flora), play an important role.

While ileitis in Japanese SAMP1/Yit mice was not evident until 20-weeks-of-age, SAMP1 mice develop robust ileitis by 10-weeks-of-age. This earlier onset of disease may point towards differences in the microbiota, although the true cause of their divergent phenotypes is unclear at the present time. Prior studies in the Fc substrain showed an inverse correlation between the presence of skin lesions and the severity of ileitis(15). We speculate that the strategy followed by Matsumoto and colleagues to breed mice with skin lesions might have resulted in delayed disease onset (~30 weeks). We show that the time course of ileitis in SAMP1, (from which the Yit strain was derived) is closer to the Fc substrain, where mice with skin lesions were not selected as breeders(10, 15). The early induction of TNF and IFN- γ mRNA transcripts in the ileum and the modest splenomegaly by 5-weeks-of-age in SAMP1 mice additionally point towards accelerated disease, compared to the SAMP1/Yit strain(5). By 10-weeks-of-age, the SAMP1 mice display transmural mixed inflammatory infiltrates and segmental hypertrophy of the muscularis propria. As disease progresses to 20-weeks-of-age, increased transmural infiltrates and villous distortion were evident. Crypt elongation and prominent goblet cell hyperplasia were also prominent pathological features. This exacerbated disease pathology also correlates with prominent expansion in cellularity of the draining mesenteric lymph node, and peripherally in the spleen, reflecting a systemic dysregulated immune response.

As reported in the SAMP1/Yit mice, we observed expansion of $CD4^+$, $CD8^+$ and $CD19^+$ lymphocyte populations in the SAMP1 strain(10, 16). Characterization of the lymphocyte populations revealed increased $\gamma\delta$ T-cell receptor subsets. As described by Kosiewicz and colleagues, $CD4^+$ lymphocytes from SAMP1/Yit mice displayed an activated phenotype with increased fractions of $CD25^+$, $CD69^+$ and $CD44^+$ (10). Here we report that SAMP1 mice similarly exhibited prominent expansion of $CD44^{high}CD62L^{low}$ effector T_{EM} and

CD44^{high}CD62L^{high} central memory T_{CM} phenotypes. This expansion appears to correlate with disease severity, as is evident by 20-weeks-of-age. As central memory T_{CM} lymphocytes express L-selectin (CD62L), they likely play a role in secondary responses and long-term memory by recirculating to secondary lymphoid organs and contributing to the perpetuation of the disease(17, 18). Conversely, effector memory T_{EM} lymphocytes, which lack L-selectin, home to effector sites (e.g. the terminal ileum) and contribute to inflammatory responses through their production of cytokines (i.e. IFN- γ , TNF)(17). Modest expansion of CD4⁺ and CD8⁺ CD44^{high} T_{EM} cells in the MLN and spleen, along with the early induction of IFN- γ and TNF suggest that at the biochemical level, the disease is already present by 5-weeks-of-age and further supports a pathogenic role of effector T-cells in the induction of ileitis in SAMP1 mice.

There appears to be a strict polarization between T_{H1} and T_{H2} cytokine phenotypes in many animal models of inflammatory bowel disease(3, 19). Prior studies have shown that the SAMP1/Yit model of ileitis shares similar pathogenic mechanisms with human CD, with predominant T_{H1} cytokine profile and CD4⁺ T-cells mediating early disease progression(3, 10). Furthermore, attenuation of SAMP1/Yit ileitis was reported by immunoneutralization of TNF and IFN- γ (12, 20). Analysis of the late ileitis in SAMP1/Yit mice revealed a role for both T_{H1} and T_{H2} cytokines during advanced disease and unexpectedly anti-IL-4 therapy ameliorated disease severity, by decreasing IFN- γ expression(12). These results highlight the synergistic balance between T_{H1} and T_{H2} cytokines during chronic mucosal inflammation and the complexity and interplay of cytokine biology in chronic models of IBD. Of note is that analysis of SAMP1/Yit cytokine expression along the time course of ileitis displayed a continuous increase of TNF and IFN- γ expression, emphasizing their role in disease progression(12, 15). Unlike the SAMP1/Yit strain, the ileitis observed in the SAMP1 mice appears to be strictly T_{H1}-polarized during disease onset, whereas T_{H2} cytokines were predominantly expressed during late disease. Thus, despite remarkably similar histopathologic features, the SAMP/Yit, the SAMP1/YitFc and the SAMP1 are not identical, with each strain presenting unique phenotypic characteristics.

A general consensus is that T_{H1} cytokines critically contribute to the pathogenesis of CD. T_{H1} responses display prominent transmural infiltration that in some cases are associated with granulomata(19). Conversely, T_{H2} mediated inflammation is characterized by a greater polymorphonuclear infiltrate and disrupted epithelial cell layer(3). This diversity in disease phenotype is evidenced by the high levels of TNF, IFN- γ and IL-12 in areas of active CD(21, 22) and further supported clinically by the nearly 70% therapeutic efficacy of TNF inhibitors (e.g. infliximab)(23). By contrast, T_{H2} cytokines are believed to play a major role in ulcerative colitis(2, 19, 24). However the clinical experience suggests that this might be a simplistic view, as evidenced by the efficacy of TNF inhibitors in 50% of patients with UC(25). A critical point is that T_{H1}-mediated inflammation may switch to T_{H2} inflammation in chronic models of IBD. This has been shown in IL-10-deficient mice, where IL-4-induced GATA-3 suppression of IL-12 signaling gradually accumulates, and ultimately a T_{H2} cytokine profile predominates(3, 26).

Of interest is the marked eosinophilic infiltration of the lamina propria in SAMP1 ileum during late disease. This observation appears to correlate with the sustained induction of IL-5 and IL-13. Increased eosinophilia and IL-5 expression have been previously reported in CD(27, 28) and both may play a role in inflammatory as well as allergic disease(29, 30). The function of IL-13 in chronic human disease is currently controversial although an increased correlation between IL-13 and ulcerative colitis has been reported(31, 32). Conversely, Inoue and colleagues report suppression of IL-13 in UC and an increase in CD (26, 33) (34). While a variety of mechanisms may be responsible, increased IL-13 production in late disease may reflect decreased negative feedback by IFN- γ (34).

In conclusion, our results strongly suggest that Crohn's disease and the chronic ileitis of SAMP1 ileitis share similar pathogenic mechanisms of disease. As in Crohn's disease, T_H1 effector and effector memory T-cells appear to be involved in early SAMP1 ileitis, likely due to systemic immune dysregulation. Large numbers of activated T cells infiltrate the intestine and draining lymphoid tissues of SAMP1 mice and patients with CD and correlate with disease severity. The hereby described distinct T_H1 and T_H2 cytokine profiles between SAMP1/Yit, SAMP1/YitFc and SAMP1 are not surprising, as these strains have been bred in isolation for over 20 years. Thus the SAMP1 mice represent an additional tool to understand critical aspects of the pathogenesis of IBD. Its dissemination to the general scientific community may greatly advance our understanding of many important aspects of CD pathogenesis.

Acknowledgments

Grant support: US PHS/NIH grants: DK067254, DK073280 to J. R.-N. US PHS/NIH grant: DK 62245 to GTF

The authors would like to thank Cheryl A. Protheroe (Mayo Clinic Arizona, Scottsdale) for major basic protein immunostaining of eosinophils.

Abbreviations

CD	Crohn's Disease
UC	Ulcerative Colitis
IBD	inflammatory bowel disease
MLN	Mesenteric lymph Node
Dex	Dexamethasone
PCR	Polymerase chain reaction
TNF	Tumor necrosis factor
CD62-L	L-Selectin

References

1. Crohn BBGL, Oppenheimer GD. Regional ileitis: A pathological and clinical entity. The Journal of American medical Association. 1932; 251:73–79.
2. Blumberg RS, Saubermann LJ, Strober W. Animal models of mucosal inflammation and their relation to human inflammatory bowel disease. *Curr Opin Immunol.* 1999; 11:648–656. [PubMed: 10631550]
3. Strober W, Fuss IJ, Blumberg RS. The immunology of mucosal models of inflammation. *Annu Rev Immunol.* 2002; 20:495–549. [PubMed: 11861611]
4. Elson CO, Sartor RB, Tennyson GS, et al. Experimental models of inflammatory bowel disease. *Gastroenterology.* 1995; 109:1344–1367. [PubMed: 7557106]
5. Matsumoto S, Okabe Y, Setoyama H, et al. Inflammatory bowel disease-like enteritis and caecitis in a senescence accelerated mouse P1/Yit strain. *Gut.* 1998; 43:71–78. [PubMed: 9771408]
6. Takeda T, Hosokawa M, Takeshita S, et al. A new murine model of accelerated senescence. *Mech Ageing Dev.* 1981; 17:183–194. [PubMed: 7311623]
7. Strober W, Nakamura K, Kitani A. The SAMP1/Yit mouse: another step closer to modeling human inflammatory bowel disease. *J Clin Invest.* 2001; 107:667–670. [PubMed: 11254665]
8. Burns RC, Rivera-Nieves J, Moskaluk CA, et al. Antibody blockade of ICAM-1 and VCAM-1 ameliorates inflammation in the SAMP-1/Yit adoptive transfer model of Crohn's disease in mice. *Gastroenterology.* 2001; 121:1428–1436. [PubMed: 11729122]

9. Lee JJ, McGarry MP, Farmer SC, et al. Interleukin-5 expression in the lung epithelium of transgenic mice leads to pulmonary changes pathognomonic of asthma. *J Exp Med*. 1997; 185:2143–2156. [PubMed: 9182686]
10. Kosiewicz MM, Nast CC, Krishnan A, et al. Th1-type responses mediate spontaneous ileitis in a novel murine model of Crohn's disease. *J Clin Invest*. 2001; 107:695–702. [PubMed: 11254669]
11. Kang SG, Piniacki RJ, Hogenesch H, et al. Identification of a chemokine network that recruits FoxP3(+) regulatory T cells into chronically inflamed intestine. *Gastroenterology*. 2007; 132:966–981. [PubMed: 17324406]
12. Bamias G, Martin C, Mishina M, et al. Proinflammatory effects of TH2 cytokines in a murine model of chronic small intestinal inflammation. *Gastroenterology*. 2005; 128:654–666. [PubMed: 15765401]
13. Madara JL, Podolsky DK, King NW, et al. Characterization of spontaneous colitis in cotton-top tamarins (*Saguinus oedipus*) and its response to sulfasalazine. *Gastroenterology*. 1985; 88:13–19. [PubMed: 2856876]
14. Brandwein SL, McCabe RP, Cong Y, et al. Spontaneously colitic C3H/HeJBir mice demonstrate selective antibody reactivity to antigens of the enteric bacterial flora. *J Immunol*. 1997; 159:44–52. [PubMed: 9200437]
15. Rivera-Nieves J, Bamias G, Vidrich A, et al. Emergence of perianal fistulizing disease in the SAMP1/YitFc mouse, a spontaneous model of chronic ileitis. *Gastroenterology*. 2003; 124:972–982. [PubMed: 12671894]
16. Olson TS, Bamias G, Naganuma M, et al. Expanded B cell population blocks regulatory T cells and exacerbates ileitis in a murine model of Crohn disease. *J Clin Invest*. 2004; 114:389–398. [PubMed: 15286805]
17. Lanzavecchia A, Sallusto F. Understanding the generation and function of memory T cell subsets. *Curr Opin Immunol*. 2005; 17:326–332. [PubMed: 15886125]
18. Sallusto F, Lenig D, Forster R, et al. Two subsets of memory T lymphocytes with distinct homing potentials and effector functions. *Nature*. 1999; 401:708–712. [PubMed: 10537110]
19. Sartor RB. Cytokines in intestinal inflammation: pathophysiological and clinical considerations. *Gastroenterology*. 1994; 106:533–539. [PubMed: 8299918]
20. Marini M, Bamias G, Rivera-Nieves J, et al. TNF-alpha neutralization ameliorates the severity of murine Crohn's-like ileitis by abrogation of intestinal epithelial cell apoptosis. *Proc Natl Acad Sci U S A*. 2003; 100:8366–8371. [PubMed: 12832622]
21. Fuss IJ, Neurath M, Boirivant M, et al. Disparate CD4+ lamina propria (LP) lymphokine secretion profiles in inflammatory bowel disease. Crohn's disease LP cells manifest increased secretion of IFN-gamma, whereas ulcerative colitis LP cells manifest increased secretion of IL-5. *J Immunol*. 1996; 157:1261–1270. [PubMed: 8757634]
22. Monteleone G, Biancone L, Marasco R, et al. Interleukin 12 is expressed and actively released by Crohn's disease intestinal lamina propria mononuclear cells. *Gastroenterology*. 1997; 112:1169–1178. [PubMed: 9098000]
23. Targan SR, Hanauer SB, van Deventer SJ, et al. A short-term study of chimeric monoclonal antibody cA2 to tumor necrosis factor alpha for Crohn's disease. Crohn's Disease cA2 Study Group. *N Engl J Med*. 1997; 337:1029–1035. [PubMed: 9321530]
24. Fiocchi C. Inflammatory bowel disease: etiology and pathogenesis. *Gastroenterology*. 1998; 115:182–205. [PubMed: 9649475]
25. Rutgeerts P, Sandborn WJ, Feagan BG, et al. Infliximab for induction and maintenance therapy for ulcerative colitis. *N Engl J Med*. 2005; 353:2462–2476. [PubMed: 16339095]
26. Spencer DM, Veldman GM, Banerjee S, et al. Distinct inflammatory mechanisms mediate early versus late colitis in mice. *Gastroenterology*. 2002; 122:94–105. [PubMed: 11781285]
27. Dubucquoi S, Janin A, Klein O, et al. Activated eosinophils and interleukin 5 expression in early recurrence of Crohn's disease. *Gut*. 1995; 37:242–246. [PubMed: 7557575]
28. Takedatsu H, Mitsuyama K, Matsumoto S, et al. Interleukin-5 participates in the pathogenesis of ileitis in SAMP1/Yit mice. *Eur J Immunol*. 2004; 34:1561–1569. [PubMed: 15162425]
29. Rothenberg ME, Mishra A, Brandt EB, et al. Gastrointestinal eosinophils. *Immunol Rev*. 2001; 179:139–155. [PubMed: 11292017]

30. Furuta GT, Forbes D, Boey C, et al. Eosinophilic gastrointestinal diseases (EGIDs). *J Pediatr Gastroenterol Nutr.* 2008; 47:234–238. [PubMed: 18664881]
31. Heller F, Florian P, Bojarski C, et al. Interleukin-13 is the key effector Th2 cytokine in ulcerative colitis that affects epithelial tight junctions, apoptosis, and cell restitution. *Gastroenterology.* 2005; 129:550–564. [PubMed: 16083712]
32. Fuss IJ, Strober W. The role of IL-13 and NK T cells in experimental and human ulcerative colitis. *Mucosal Immunol.* 2008; 1 (Suppl 1):S31–33. [PubMed: 19079225]
33. Inoue S, Matsumoto T, Iida M, et al. Characterization of cytokine expression in the rectal mucosa of ulcerative colitis: correlation with disease activity. *Am J Gastroenterol.* 1999; 94:2441–2446. [PubMed: 10484006]
34. Vainer B, Nielsen OH, Hendel J, et al. Colonic expression and synthesis of interleukin 13 and interleukin 15 in inflammatory bowel disease. *Cytokine.* 2000; 12:1531–1536. [PubMed: 11023669]

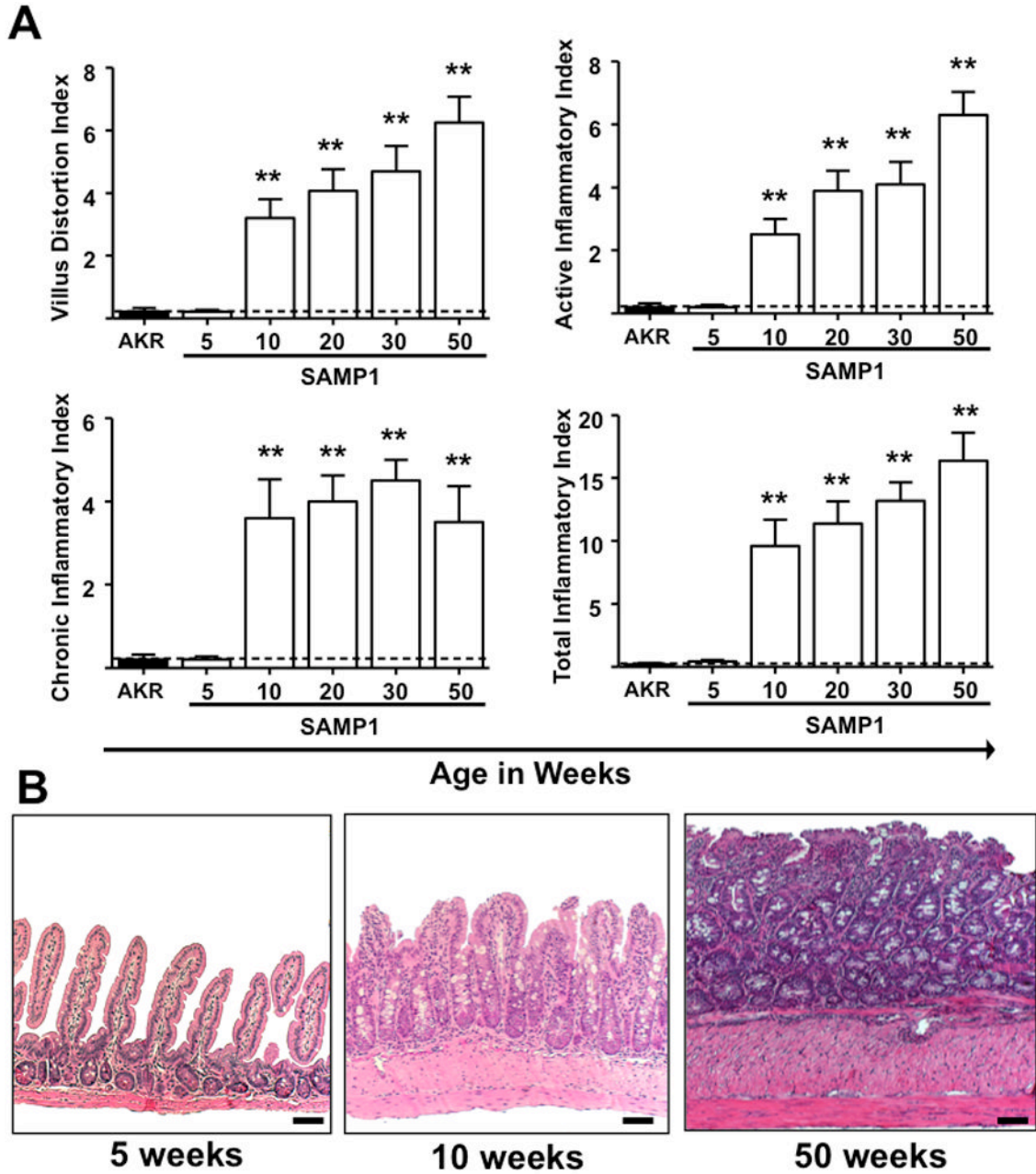


Figure 1. Time course and histological features of ileitis in SAMP1 mice

Inflammatory indices (Villus distortion, active, chronic and total) were assessed by a pathologist (PJ) in a blinded fashion using a previously described scoring system, from 5- to 50-weeks-of-age. Normal villus, crypt and muscularis architecture was evident at 5-weeks-of-age. At 10-weeks-of age, transverse mixed inflammatory infiltrates; goblet and crypt hyperplasia and hypertrophy of the muscularis propria were present. Further progression of transverse infiltrates, villus distortion and muscularis hypertrophy were observed in 20- to 50-week-old mice with additional crypt elongation and prominent goblet cell hyperplasia. Scale bars represent 100µm. Data expressed as mean \pm SEM, ** $P < .01$ vs. total mean \pm SEM for age-matched AKR controls from 5- to 50-weeks-of-age (n=5–9/age group).

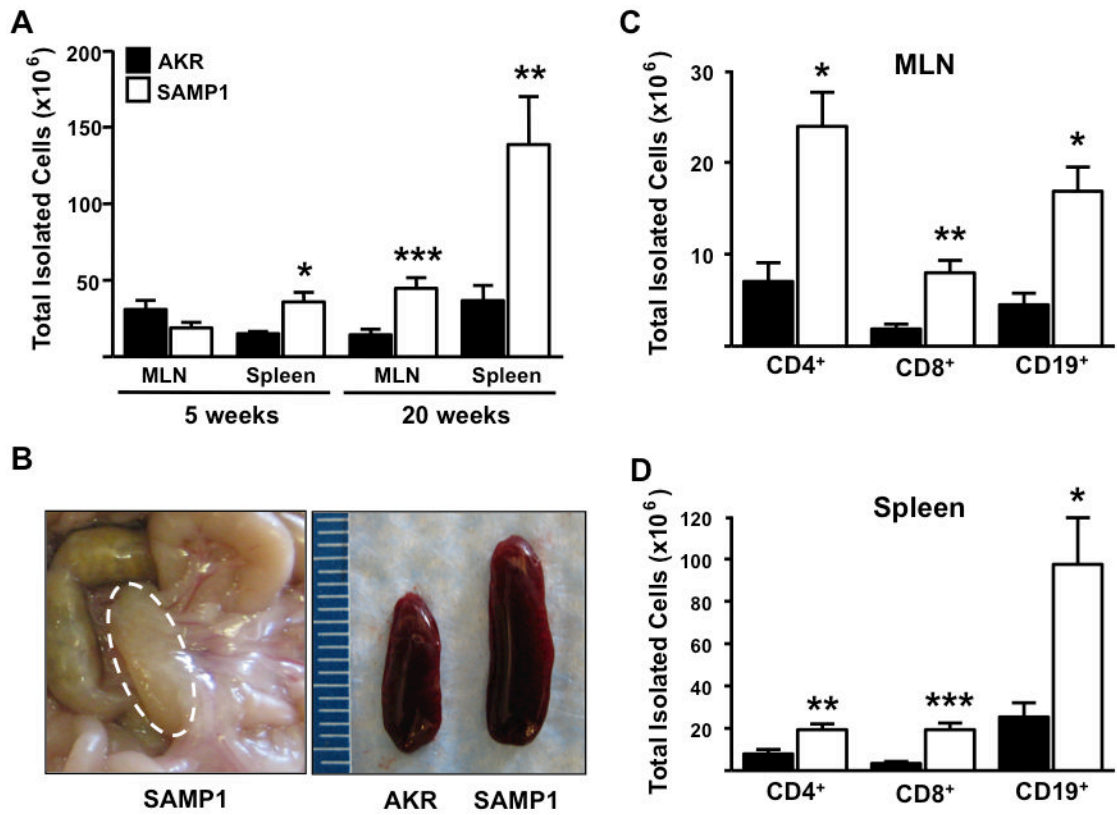


Figure 2. Expansion of lymphoid compartments and lymphocyte subsets in SAMP1 mice (A & B) Lymphoid compartments (MLN and spleen) of SAMP1 mice displayed increased size and cellularity compared to uninflamed AKR controls. (B) Representative pictures show SAMP1 MLN and spleen of indicated strains at 20-weeks-of-age. (C & D) Flow cytometric analyses revealed expansion of indicated lymphocyte subsets. (A.) Data expressed as mean \pm SEM, * $P < .05$, ** $P < .01$, *** $P < .001$ (C & D) vs. 20-weeks-of-age AKR control (n=6/strain).

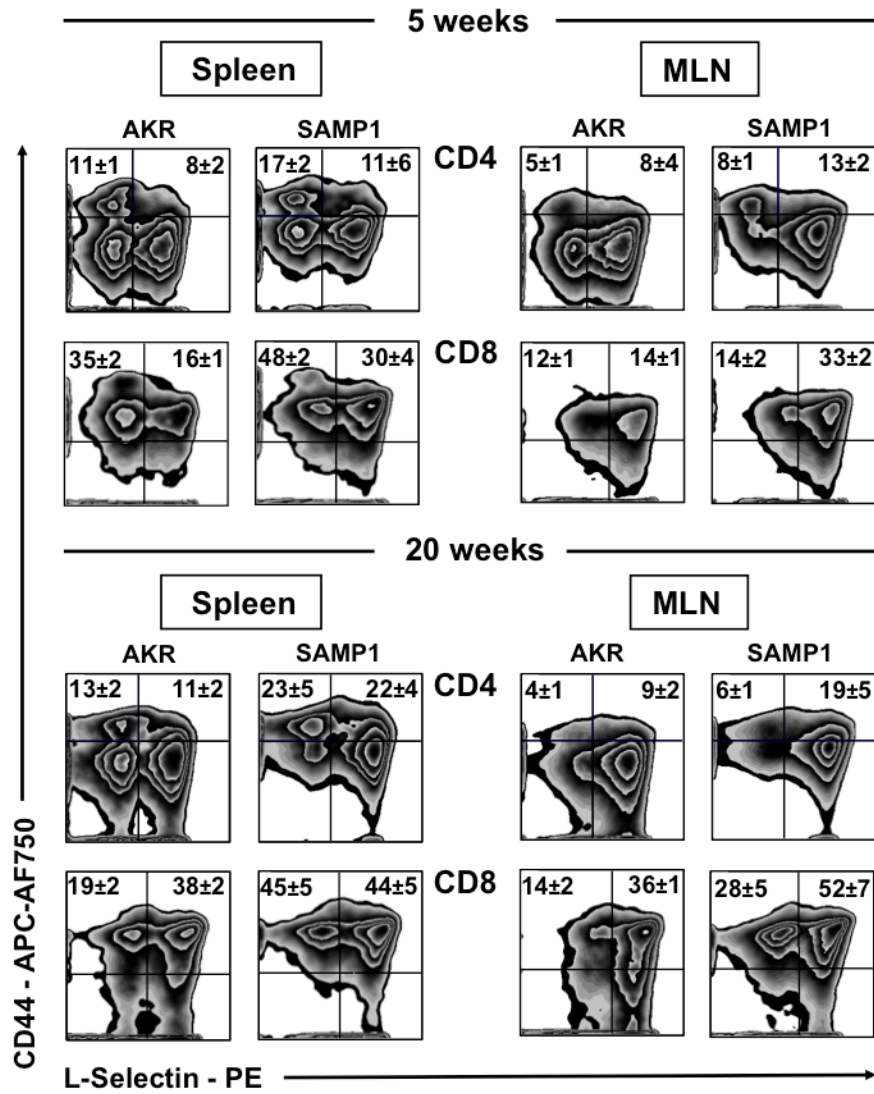


Figure 3. Expansion of effector (T_{EM}) and central memory T-lymphocytes (T_{CM}) in SAMP1 mice

Flow cytometric analyses of SAMP1 and AKR mice MLN and spleen displayed expansion of effector T_{EM} (CD44^{high}CD62L^{low}) and central memory (CD44^{high}CD62L^{high}) T_{CM} CD4⁺ and CD8⁺ T-lymphocytes. Representative zebra plots gated on forward and side scatter, CD4⁺ and CD8⁺ were obtained from cells isolated from indicated organs at 5- and 20-weeks-of-age (n=4–6/strain).

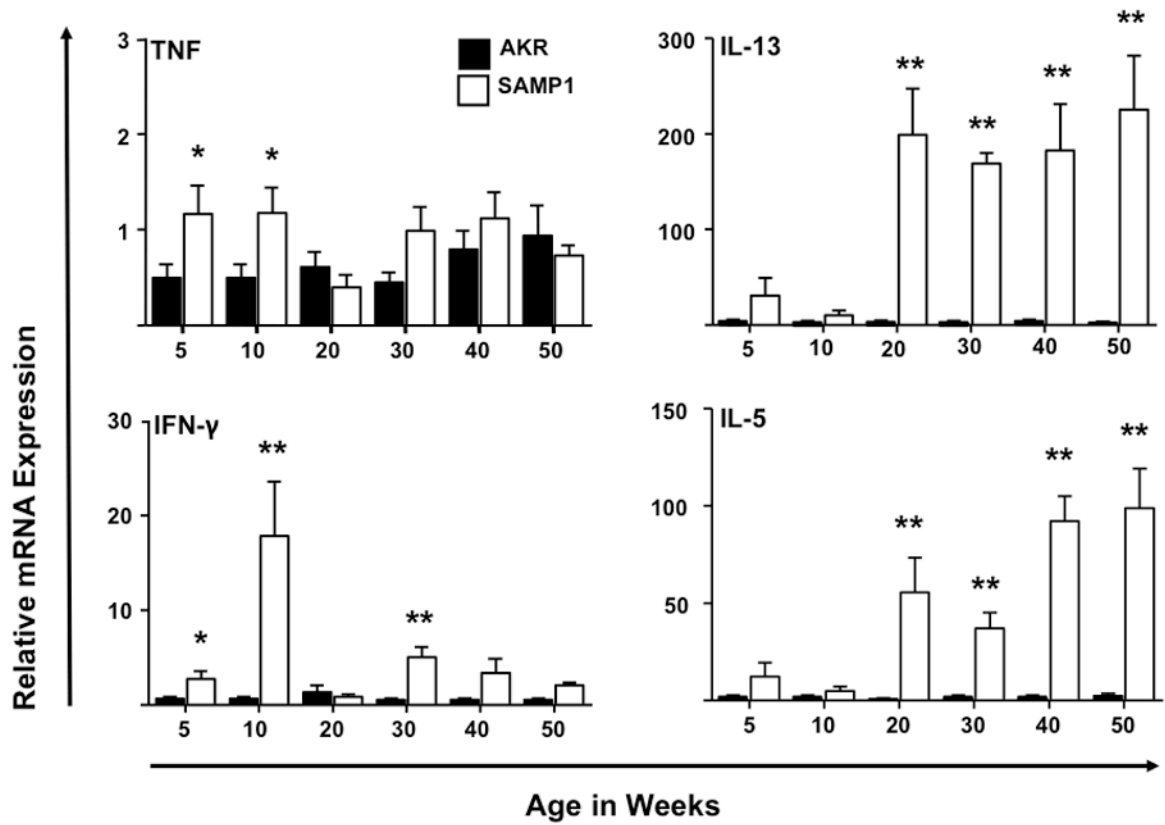


Figure 4. Differential ileal cytokine expression profiles during early and late SAMP1 ileitis
 Relative mRNA expression of indicated cytokines along the time course of the disease were evaluated in ilea of AKR and SAMP1 mice. Increased TNF, IFN- and IL-10 transcripts were observed at 5- to 10-weeks-of age while IL-5, IL-13 expression peaked at 20-weeks-of age and remain elevated thereafter. Target cytokines were normalized to 18S ribosomal RNA. Data expressed as means \pm SEM, * $P < .05$, ** $P < .01$ vs. Age-matched AKR control (n=5–6/strain).

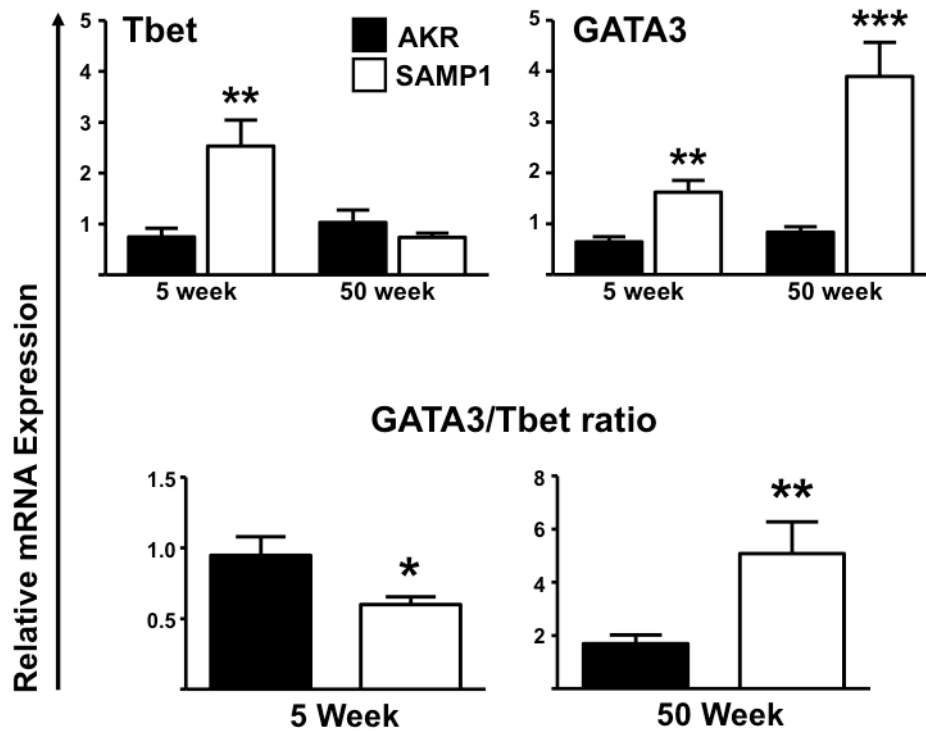


Figure 5. Differential ileal cytokine transcription factor expression profiles during early and late SAMP1 ileitis

Tbet (T_H1) and GATA3 (T_H2) relative mRNA expression was assessed during early and late disease. GATA3/Tbet ratio represents the GATA3 and Tbet mRNA ratio of SAMP1 compared to uninfamed AKR control mice at 5- and 50-weeks-of-age. Target transcription factors were normalized to 18S ribosomal RNA. Data expressed as means \pm SEM, * $P < .05$, ** $P < .01$ vs. age-matched AKR control (n=5–6/strain).

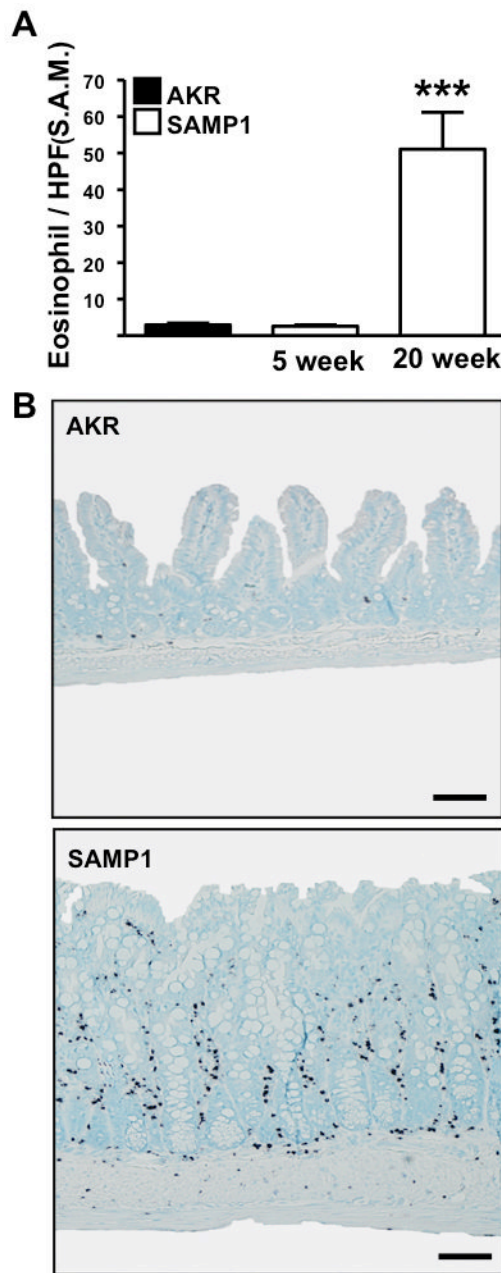


Figure 6. Increased eosinophilic infiltration of the chronically inflamed SAMP1 ileum
 (A) Eosinophilic infiltration of the ileal lamina propria was assessed by immunostaining for MBP during early and late ileitis in SAMP1 mice and AKR mice (n=5). Data expressed as means \pm SEM, ***P<.001 vs. 5-week-old SAMP1. (B) Representative MBP immunostaining of indicated strains at 20-weeks-of-age, scale bars represent 100 μ m.

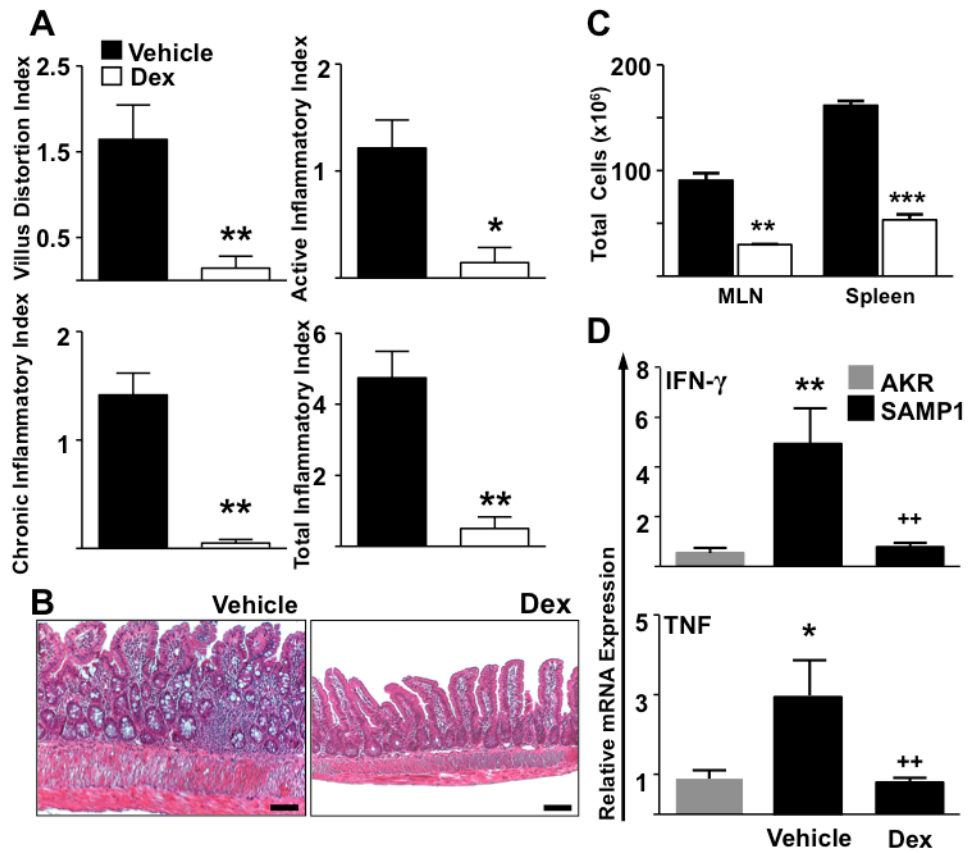


Figure 7. Corticosteroid therapy attenuated ileitis, decreased lymphoid organ cellularity and TH1 cytokine transcripts in ilea of SAMP1 mice

(A & B) Dexamethasone administration (100 μ g, I.P., Q.O.D. over 8 days) attenuated disease indices and restored intestinal architecture in 11-week-old SAMP1 mice compared to age-matched saline-treated (vehicle) controls. (C) The cellularity of the MLN and spleen as well as (D) IFN- and TNF ileal mRNA expression were additionally decreased. Target cytokines were normalized to 18S ribosomal RNA. Data expressed as means \pm SEM, *P<0.05, **P<.01, ***P<.001 vs. age-matched AKR control, ++P<.01 vs. Vehicle treated SAMP1. Scale bars represent 100 μ m (A & C; n=6-7, D; n=3)

Table 1
Expansion of CD4⁺ and CD8⁺ T-cell subsets in the MLN and spleen of SAMP1 mice

Absolute counts calculated by correcting the cellularity of the lymphoid compartments by the percentage of cells expressing indicated T cell receptors at 20-weeks-of-age.

MLN			
Phenotype	AKR	SAMP1/SkuSIc	P value
CD4 ⁺	7.8 ± 0.6	26.5 ± 1.3	P<0.0001
CD8 ⁺	1.0 ± 0.2	5.4 ± 1.0	P=0.007
Spleen			
Phenotype	AKR	SAMP1/SkuSIc	P value
CD4 ⁺	8.0 ± 1.7	25 ± 2.0	P=0.005
CD8 ⁺	1.5 ± 2.0	11 ± 1.0	P=0.001

Data expressed as mean percentage cellularity ± SEM, (student *t*-test; n=6)